PHILOSOPHICAL TRANSACTIONS OF THE ROYAL SOCIETY A MATHEMATICAL, PHYSICAL & ENGINEERING SCIENCES

Finite–element model updating using experimental test data: parametrization and regularization

Michael I. Friswell, John E. Mottershead and Hamid Ahmadian

Phil. Trans. R. Soc. Lond. A 2001 **359**, 169-186
doi: 10.1098/rsta.2000.0719

10.1098/rsta.2000.0719

THE ROYAL SOCIETY

Finite-element model updating using experimental test data: parametrization and regularization

By Michael I. Friswell[1], John E. Mottershead[2] and Hamid Ahmadian[3]

[1]*Department of Mechanical Engineering, University of Wales Swansea, Swansea SA2 8PP, UK*
[2]*Department of Engineering, University of Liverpool, Liverpool L69 3BX, UK*
[3]*Department of Mechanical Engineering, Iran University of Science and Technology, Narmak, Tehran, Iran*

Two critical issues in model updating are deciding how a finite-element model should be parametrized and estimating the unknown parameters from the resulting ill-conditioned equations. A lack of understanding of these issues will lead to updated models without physical meaning. This paper outlines the authors' approach to parametrization, using physical, geometric and generic element parameters. It also applies useful methods of regularization, namely parameter constraints, the singular-value decomposition, L-curves and cross-validation to model updating.

Keywords: updating; finite element; vibration test; parameters; regularization

1. Introduction

Finite-element model updating has become a viable approach to increase the correlation between the dynamic response of a structure and the predictions from a model. In model updating, parameters of the model are adjusted to reduce a penalty function based on residuals between a measurement set and the corresponding model predictions. Typical measurements include the modal model (natural frequencies and mode shapes) and the frequency response functions. The choice of penalty function, and also the optimization approach, has been the subject of much research and is well covered by the authors' survey paper (Mottershead & Friswell 1993), book (Friswell & Mottershead 1995) and special issue of *Mechanical Systems and Signal Processing* (Mottershead & Friswell 1998). This paper considers the issues of how to parametrize a finite-element model and how to regularize the resulting estimation equations to obtain a well-conditioned solution. These are critical issues in model updating.

2. Parametrization of the finite-element model

Parametrization is a key issue in finite-element model updating. It is important that the chosen parameters should be able to clarify the ambiguity of the model, and in that case it is necessary for the model output to be sensitive to the parameters. Usually elements in the mass and stiffness matrices perform very poorly as candidate

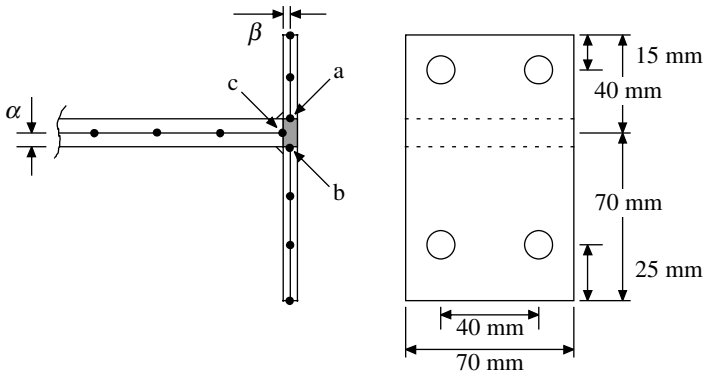

Figure 1. Modelling of the welded joint.

parameters, and this is one reason why the direct methods of model updating are not favoured (Friswell & Mottershead 1995). One reason for this poor performance is that the stiffness matrix element values are dominated by the high-frequency modes, whereas the low-frequency modes are measured. Element parameters, such as the flexural rigidity of a beam element, may be used provided there is some justification as to why the element properties should be in error. Mottershead *et al*. (1996) used geometric parameters, such as beam offsets, for the updating of mechanical joints and boundary conditions. Gladwell & Ahmadian (1995) and Ahmadian *et al*. (1997*a*) demonstrated the effectiveness of parametrizing the modes at the element level, and used both geometric parameters and element-modal parameters (i.e. the so-called generic element method) to update mechanical joints. The following subsections will concentrate on the modelling of joints, since these are often the most difficult areas of a structure to model.

(*a*) *Physical and geometric parameters*

There are a number of physical parameters of a joint that could be updated. A beam with a flange welded as a T-joint, shown in figure 1, will be taken as an example. The beam part was of length 0.4 m and cross-section 70 mm × 12 mm. The flange area was 110 mm × 70 mm and the thickness of the flange was 6 mm. Pairs of bolt holes, diameter 12 mm and 40 mm apart, were drilled 25 mm from the edge of the longer part of the flange and 15 mm from the edge of the shorter part of the flange, as shown in figure 1. Only vibration in a single plane was considered. The resonances of the structure are lightly damped and well separated, making natural frequency identification and mode shape pairing straightforward.

The beam structure was modelled with cubic beam elements for the transverse motion and linear bar extension elements. The nodes possess axial and transverse translation degrees of freedom together with a rotation in the same plane. The beam was represented by eight elements, the flange was represented by five elements, and nodes were located to coincide with the bolt holes. The shaded area is considered rigid and is enforced by a constraint matrix linking nodes a, b and c. Only the degrees of freedom corresponding to node c are independent and included in the model. The mass and inertia of the rigid area were lumped at node c.

One approach to updating this joint is to alter the beam stiffness of the elements closest to the joint. Although this often gives good results, the model error is not

Table 1. *Natural frequencies* (Hz) *for the welded joint in the beam*

	free–free						clamped–free			
measured	324	823	1243	1975	3022	3898	56	354	986	1523
initial	318	813	1212	1940	2976	3833	55	349	972	1504
updated	325	827	1235	1978	3023	3897	56	356	989	1525

Table 2. *Updated parameters for the welded joint in the beam*

	α (mm)	β (mm)	thickness change (%)
initial	6.0	3.0	—
updated	6.4	3.0	−3.2

localized at the joint, but is spread through the updated elements. Flexibility may be introduced into the rigid area by using discrete translational and rotary springs between nodes a, b and c. Mottershead *et al*. (1996) showed that for typical joints the structure's response is insensitive to the stiffness of these discrete springs, and such insensitivity causes great problems for the updating algorithms. A powerful alternative is to update geometric parameters, for example the offset of nodes b and c from node a, denoted by α and β in figure 1. The offset parameters have a physical meaning with regard to stiffness updating: the shaded (rigid) region in figure 1 can be considered to expand or contract depending upon whether the offset dimensions are extended or reduced by updating. The offset dimensions are assumed to affect only the stiffness matrix; the mass matrix is unaffected. A third parameter, the variation in the thickness of the beam and flange, was used to allow for a global shift in all the modelled natural frequencies. The beam was tested twice: under free–free conditions and clamped at the flanges. Updating was carried out using both sets of natural frequency data, using a sensitivity-based approach (Mottershead *et al*. 1996). Mode shape data were measured but only the natural frequencies were used for updating. The mode shape data were used to check the pairing of the experimental and analytical modes, although since the natural frequencies were well separated (and the structure basically one dimensional), this task is straightforward. The spatial incompleteness of the measured modes is not an issue here because the number of parameters has been reduced using physical reasoning, resulting in an overdetermined identification problem. Table 1 shows the measured, and initial and updated analytical natural frequencies, and table 2 shows the initial and updated parameter values. The natural frequencies are much improved after updating. The beam thickness only changes by *ca*. 3%, which is within the measurement tolerance for the beam thicknesses.

(*b*) *Generic parameters*

Gladwell & Ahmadian (1995) and Ahmadian *et al*. (1997*b*) introduced the generic element approach. The method depends on the eigenvalue decomposition of stiffness

and mass matrices at the element level, or substructure masses and stiffnesses typically at a joint. The joint would then be updated by adjusting a set of parameters related to its own eigenvalues and eigenvectors. It would be possible, for example, to update parameters related to the bending behaviour in a particular mode of a joint while retaining the original stiffness of the other modes. Model correction using submodel coefficients or physical parameters (such as Young's modulus or the thickness of a beam) can be restrictive and may lead to converged models whose physical interpretation does not match the real structure. The generic element approach is equivalent to modifying the coefficients in the element shape-function equations but not the order of the shape functions. Generic elements are based on the element (or substructure) free–free modes but other coordinate systems are possible of course, and might have advantages for particular updating problems.

The mass matrix of a substructure, such as a joint, is assumed to be correct. The substructure stiffness matrix may be decomposed as

$$\boldsymbol{K}^{\mathrm{s}} = \boldsymbol{V}_0 \varLambda_0 \boldsymbol{V}_0^{\mathrm{T}}, \tag{2.1}$$

where $\varLambda_0$ and $\boldsymbol{V}_0$ are the eigenvalues and unit normalized eigenvectors (mode shapes) of the stiffness matrix. Assuming that the corrected eigenvectors are given by a transformation,

$$\boldsymbol{V} = \boldsymbol{V}_0 \boldsymbol{R}, \tag{2.2}$$

where $\boldsymbol{R}$ is an orthogonal matrix, and letting the eigenvalues vary, gives the updated substructure stiffness matrix as

$$\boldsymbol{K}^{\mathrm{su}} = \boldsymbol{V}_0 \boldsymbol{R} \varLambda \boldsymbol{R}^{\mathrm{T}} \boldsymbol{V}_0^{\mathrm{T}}, \tag{2.3}$$

or with three strain modes,

$$\boldsymbol{K}^{\mathrm{su}} = \boldsymbol{V}_0 \begin{bmatrix} \kappa_{11} & \kappa_{12} & \kappa_{13} \\ & \kappa_{22} & \kappa_{23} \\ \mathrm{sym} & & \kappa_{33} \end{bmatrix} \boldsymbol{V}_0^{\mathrm{T}}. \tag{2.4}$$

The six terms $\kappa_{11}, \ldots, \kappa_{33}$ are available for updating. If only the diagonal terms—κ_{11}, κ_{22} and κ_{33}—are changed, then this amounts to changing the natural frequencies of the substructure strain modes while keeping the mode shapes unaltered. These generic parameters have a meaning in terms of the interaction between the physical modes, which is especially important if substructures are related through constraints. However, note that the updated generic parameters cannot be interpreted in terms of physical parameters of the substructure.

As an example, consider the out-of-plane vibration of the frame structure shown in figure 2. Figure 3 shows the substructure types for the frame, namely a connecting element and the L- and T-shaped joints. Although each of these substructures could be updated using generic parameters, generic parameters relating to elements will be updated here. Figure 3 also shows the five elements that will be used in the updating. Each of the beam or bar elements has three rigid-body modes and three strain modes. The strain modes have the form

$$\boldsymbol{V}_0^{\mathrm{T}} = \begin{bmatrix} 0 & \beta & 0 & 0 & -\beta & 0 \\ 0 & 0 & \beta & 0 & 0 & -\beta \\ 2\delta & 0 & -\delta & -2\delta & 0 & -\delta \end{bmatrix}, \tag{2.5}$$

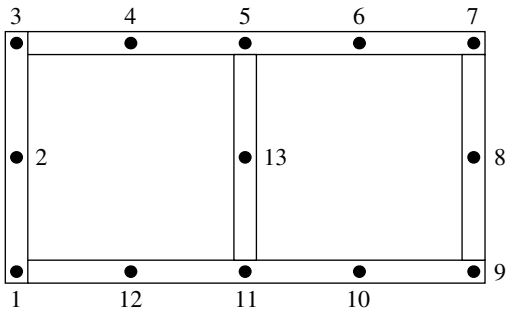

Figure 2. The frame structure: out-of-plane vibration is considered.

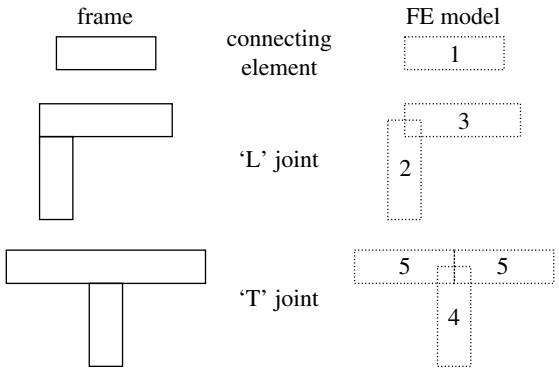

Figure 3. Element types for the frame exampe: the numbers represent the element groups.

where $\beta = 1/\sqrt{2}$, $\delta = 1/(l\sqrt{10})$ and l is the element length. The ordering of the degrees of freedom in (2.5) will change with the orientation of the element if a global coordinate system is used. Physically, (2.5) gives the modes in order of eigenvalue magnitude, where the first mode is a bending mode that merely involves rotation but no displacement at the nodes, the second is purely torsional, and the last is also a bending mode but involves both rotation and displacement at the nodes. Thus the first two modes are antisymmetric and the third mode is symmetric.

The number of parameters in the frame example is large. Just considering elements adjacent to the joints gives 14 elements, each with 6 generic parameters. Updating these 84 parameters produces ill-conditioned equations that require regularization. Hence this example will be used later to demonstrate the regularization methods.

(*c*) *Equivalent models*

Occasionally part of the structure is so ill-defined that no finite-element model can be constructed with confidence. Common examples are welded joints in frames and in structures such as automobile bodies. The example considered here is the rubber seal which provides the connection between a vehicle window and the car body structure. The seal has a complicated cross-sectional shape into which the window glass and the steel sheet are pressed to form the joint. Furthermore, it is important to model the seal accurately because vibration of the window has a strong influence on the acoustics of the passenger compartment. In such cases there seems to be no reasonable alternative to *direct* parameter estimation.

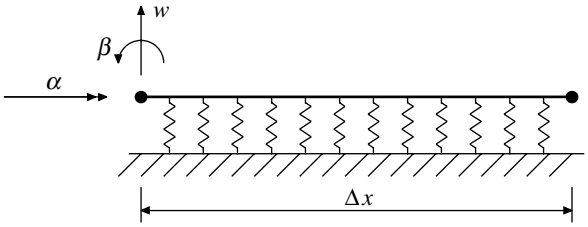

Figure 4. The rubber seal equivalent element.

The glass and the body panels are regularly modelled with plate elements having 3 degrees of freedom at each node. Thus, the equivalent rubber seal (ERS) element should have the same degrees of freedom at each node. In its most general form, the element is chosen to have 4 nodes and 12 degrees of freedom. The tests on the seal were performed with a very stiff foundation that was assumed to be rigid in the model. Although this is not the configuration in which the seal operates in the vehicle, Ahmadian *et al.* (1997*b*) showed that by using the various physical constraints and the symmetry of the element, the model of the seal may be derived from measurements on the rigid foundation.

Figure 4 shows the seal model in the experimental configuration. Essentially there are two unknown parameters, denoted k_w and k_α, that relate to a distributed bending and torsional stiffness per unit length. The stiffness matrix can be calculated by ensuring that the displacement function within the seal matches the cubic displacement function along the edge of the plate, and assuming that the torsional and bending motions decouple. Based on the displacements $(w_1,\ \Delta x\,\beta_1,\ w_2,\ \Delta x\,\beta_2)$, the bending stiffness is

$$\frac{k_w\,\Delta x}{420}\begin{bmatrix} 156 & -22 & 54 & 13 \\ & 4 & -13 & -3 \\ & & 156 & 22 \\ \text{sym} & & & 4 \end{bmatrix}, \tag{2.6}$$

where Δx is the length of the seal element. This stiffness matrix has the same form as the mass matrix of the standard Euler–Bernoulli beam element because the stiffness is assumed to be distributed. Now use Δy to represent the width of the plate element associated with the seal element. Then based on the displacements $(\Delta y\,\alpha_1, \Delta y\,\alpha_2)$, the torsional stiffness is

$$\frac{k_\alpha\,\Delta x}{420}\begin{bmatrix} 156 & 54 \\ \text{sym} & 156 \end{bmatrix}. \tag{2.7}$$

The glass used in the experiment was rectangular, which is not typical of a car window, but the rubber seal was of the type used in modern vehicles. The seal was mounted in a rigid frame. The glass plate (dimensions 0.5 m × 0.8 m × 0.0025 m) was modelled with a mesh of 5 × 8 plate elements, which was sufficient to eliminate the discretization error in the first 10 modes of vibration. The rubber seal was modelled by using 26 elastic support elements. The parameters k_w and k_α were obtained by minimizing the error between the measured natural frequencies and the finite-element prediction; the results are given in table 3. The mode shapes were used to ensure the correct pairing of the modes, but were not used in the identification. The greatest

Table 3. *Measured and identified natural frequencies* (Hz) *for the equivalent rubber seal*

mode	measured	predicted 5×8 mesh	predicted 10×16 mesh
1	30.39	33.79	33.76
2	65.17	65.54	65.49
3	111.21	112.14	112.01
4	118.84	114.98	114.92
5	139.94	140.39	140.28
6	181.27	183.63	183.52
7	184.23	187.30	187.38
8	229.91	236.25	235.70
9	234.91	252.61	252.94
10	263.68	262.55	261.95

error occurs in the first natural frequency and has been attributed to the dynamics of the experimental rig, which is supposed to provide a rigid boundary constraint but behaves like a rigid-body mode at very low frequencies because of its large mass. Almost identical results were obtained when the mesh was refined to 10×16, as shown in table 3.

New measurements were obtained when the glass was replaced by a steel plate, and these measurements were compared with predictions from the previously identified models, but with the plate elements given the properties of steel. The results (table 4) indicate that the identified seal parameters have physical meaning, otherwise the excellent agreement between the measured and predicted results is unlikely to have been achieved. The agreement shows that the discretization error in the rubber seal model has the same order or is smaller than the error in the plate element.

3. Regularization

The treatment of ill-conditioned, noisy systems of equations is a problem central to finite-element model updating; Ahmadian *et al.* (1998) gave further details. Such equations often arise in the correction of finite-element models by using vibration measurements. The regularization problem centres around the linear equation

$$\boldsymbol{A}\theta = \boldsymbol{b}, \tag{3.1}$$

where θ is a vector of the m parameter changes we wish to determine, and $\boldsymbol{b}$ is a vector of n residual quantities derived from the measured data and the current estimate of the model. In model updating, the relationship between the measured output (e.g. natural frequencies, mode shapes, or the frequency response function) is generally nonlinear. In this case the problem is linearized using a Taylor series expansion and iteration performed until convergence. When $\boldsymbol{b}$ is contaminated with additive, independent random noise with zero mean, it is well known that the least-squares solution, θ_{LS}, is unique and unbiased provided that $\mathrm{rank}(\boldsymbol{A}) = m$. When $\boldsymbol{A}$ is close to being rank deficient, then small levels of noise may lead to a large deviation in the estimated parameters from their exact values. The solution is said to be unstable and (3.1) is ill-conditioned.

Table 4. *Measured and identified natural frequencies* (Hz) *for the equivalent rubber seal with a steel plate*

mode	measured	predicted 5×8 mesh	predicted 10×16 mesh
1	29.61	32.71	32.69
2	60.42	59.63	59.62
3	98.89	101.69	101.61
4	106.23	104.19	104.23
5	120.14	126.34	126.38
6	155.39	165.56	165.65
7	164.13	167.22	167.61
8	209.26	211.14	210.64
9	228.44	223.94	224.77
10	233.90	232.87	232.50

A different problem occurs when $m > n$, so that (3.1) is underdetermined and there are an infinite number of solutions. The Moore–Penrose pseudo-inverse in the form

$$\theta_{\mathrm{LS}} = \boldsymbol{A}^{\mathrm{T}}[\boldsymbol{A}\boldsymbol{A}^{\mathrm{T}}]^{-1}\boldsymbol{b} \tag{3.2}$$

provides the solution of minimum norm, as does singular-value decomposition (SVD). For the case when $\mathrm{rank}(\boldsymbol{A}) = r < \min(m, n)$, the SVD will again result in the minimum norm solution. This is a form of regularization which has been widely applied in the model updating community. Unfortunately, minimum norm solutions rarely lead to physically meaningful updated parameters.

One solution to the problem of ill-conditioning is to select only a subset of the parameters for updating (Friswell *et al*. 1998). The parameters that are chosen are those to which the response data are sensitive, but the parameters must also be able to correct the errors in the model. This choice is generally determined by the process of subset selection, whereby candidate subsets of parameters are tested and the resulting response residual evaluated. For a given number of parameters, the subset with the smallest residual is chosen. Clearly, the number of potential parameter subsets grows rapidly and sub-optimal methods must be used for practical problems.

(*a*) *Side constraints*

Model updating often leads to an ill-conditioned parameter estimation problem, and an effective form of regularization is to place constraints on the parameters. One constraint could be that the deviation between the parameters of the updated model and the initial model are minimized; another could be that differences between parameters could be minimized. For example, in a frame structure a number of T-joints may exist that are nominally identical. Due to manufacturing tolerances the parameters of these joints will be slightly different, although these differences should be small. Therefore, a side constraint is placed on the parameters, so that both the residual and the differences between nominally identical parameters are minimized. Thus if (3.1) generates the residual, the parameter is sought which minimizes the

quadratic cost function

$$J(\theta) = \|\boldsymbol{A}\theta - \boldsymbol{b}\|^2 + \lambda^2\|\boldsymbol{C}\theta - \boldsymbol{d}\|^2, \tag{3.3}$$

for some matrix $\boldsymbol{C}$, vector $\boldsymbol{d}$ and regularization parameter λ. The regularization parameter is chosen to give a suitable balance between the residual and the side constraint. For example, if there were only two parameters, which were nominally equal, then

$$\boldsymbol{C} = [1 \ -1], \qquad \boldsymbol{d} = \{0\}. \tag{3.4}$$

Minimizing (3.3) is equivalent to minimizing the residual of

$$\begin{bmatrix} \boldsymbol{A} \\ \lambda\boldsymbol{C} \end{bmatrix} \theta = \begin{Bmatrix} \boldsymbol{b} \\ \lambda\boldsymbol{d} \end{Bmatrix}. \tag{3.5}$$

Equation (3.5) then replaces (3.1), although with the significant difference that (3.5) is generally overdetermined, whereas (3.1) is often underdetermined. The constraints should be chosen to satisfy Morozov's complementation condition

$$\operatorname{rank} \begin{bmatrix} \boldsymbol{A} \\ \boldsymbol{C} \end{bmatrix} = m, \tag{3.6}$$

which ensures the coefficient matrix in (3.5) is full rank.

(*b*) *The singular-value decomposition*

The SVD of $\boldsymbol{A}$ may be written in the form

$$\boldsymbol{A} = \boldsymbol{U}\boldsymbol{\Sigma}\boldsymbol{V}^{\mathrm{T}} = \sum_{i=1}^{m} \sigma_i \boldsymbol{u}_i \boldsymbol{v}_i^{\mathrm{T}}, \tag{3.7}$$

where $\boldsymbol{U} = [\boldsymbol{u}_1\boldsymbol{u}_2 \ldots \boldsymbol{u}_n]$ and $\boldsymbol{V} = [\boldsymbol{v}_1\boldsymbol{v}_2 \ldots \boldsymbol{v}_m]$ are $n \times n$ and $m \times m$ orthogonal matrices, and

$$\boldsymbol{\Sigma} = \operatorname{diag}(\sigma_1, \sigma_2, \ldots, \sigma_m), \tag{3.8}$$

where the singular values, σ_i, are arranged in descending order ($\sigma_1 \geqslant \sigma_2 \geqslant \cdots \geqslant \sigma_m$). In ill-posed problems, two commonly occurring characteristics of the singular values have been observed: the singular values decay steadily to zero with no particular gap in the spectrum; and the left and right singular vectors $\boldsymbol{u}_i$ and $\boldsymbol{v}_i$ tend to have more sign changes in their elements as the index i increases.

The solution for the parameters using the SVD is

$$\theta = \sum_{i=1}^{m} \frac{\boldsymbol{u}_i^{\mathrm{T}}\boldsymbol{b}}{\sigma_i}\boldsymbol{v}_i. \tag{3.9}$$

Thus the components of $\boldsymbol{A}$ corresponding to the low singular values have only a small contribution to $\boldsymbol{A}$ but a large contribution to the estimated parameters. The elements of these singular vectors (corresponding to the low singular values) are also generally highly oscillatory. Equation (3.9) shows that the noise will be amplified when $\sigma_i < \boldsymbol{u}_i^{\mathrm{T}}\boldsymbol{b}$, and this may be used to decide where to truncate the singular values.

If $\boldsymbol{A}$ does not contain noise, then the singular values will decay to zero whereas the $\boldsymbol{u}_i^{\mathrm{T}}\boldsymbol{b}$ terms will decay to the noise level. Ahmadian *et al*. (1998) and Hemez & Farhat (1995) consider this approach in more detail.

The standard SVD is incapable of taking account of the side constraint, as this requires the generalized SVD. Space does not permit a full explanation of the generalized SVD, and the reader is referred to Hansen (1994) for more complete detail of the decomposition. In equation (3.5), $\boldsymbol{A}$ and $\boldsymbol{C}$ are decomposed as

$$\boldsymbol{A} = \boldsymbol{U}\begin{bmatrix}\boldsymbol{I} & \boldsymbol{0}\\ \boldsymbol{0} & \boldsymbol{\Sigma}\end{bmatrix}\boldsymbol{X}^{-1}, \qquad \boldsymbol{C} = \boldsymbol{V}\begin{bmatrix}\boldsymbol{0} & \boldsymbol{M}\end{bmatrix}\boldsymbol{X}^{-1}, \tag{3.10}$$

where $\boldsymbol{X}$ is a non-singular $m\times m$ matrix. $\boldsymbol{U}$ and $\boldsymbol{V}$ are $n\times m$ and $p\times p$, respectively, and their columns are orthogonal (but they are not related to the matrices $\boldsymbol{U}$ and $\boldsymbol{V}$ of the standard SVD) and $n \geqslant m \geqslant p$. The matrices $\boldsymbol{\Sigma}$ and $\boldsymbol{M}$ are

$$\boldsymbol{\Sigma} = \mathrm{diag}(\sigma_1, \sigma_2, \ldots, \sigma_p), \qquad \boldsymbol{M} = \mathrm{diag}(\mu_1, \mu_2, \ldots, \mu_p), \tag{3.11}$$

where $1 \geqslant \sigma_1 \geqslant \sigma_2 \geqslant \cdots \geqslant \sigma_p \geqslant 0$ and $0 \leqslant \mu_1 \leqslant \mu_2 \leqslant \cdots \leqslant \mu_p \leqslant 1$, and σ_i and μ_i are normalized so that

$$\sigma_i^2 + \mu_i^2 = 1. \tag{3.12}$$

In decreasing order, the p generalized singular values of $\begin{bmatrix}\boldsymbol{A}\\ \boldsymbol{C}\end{bmatrix}$ are

$$\gamma_i = \frac{\sigma_i}{\mu_i}. \tag{3.13}$$

The solution to (3.5) can then be expressed as

$$\theta = \sum_{i=1}^{p} \frac{\gamma_i^2}{\gamma_i^2 + \lambda^2}\frac{\boldsymbol{u}_i^{\mathrm{T}}\boldsymbol{b}}{\sigma_i}\boldsymbol{v}_i + \sum_{i=p+1}^{m}(\boldsymbol{u}_i^{\mathrm{T}}\boldsymbol{b})\boldsymbol{v}_i. \tag{3.14}$$

The regularization parameter, λ, has the effect of damping the effect of the lower singular values (lower than about λ) and thus smoothing the solution. The expansion in terms of the SVD (3.14) may also be used to specify a solution as a truncated SVD. If, instead of specifying λ, the series is truncated by keeping only the largest k singular values, then the solution is

$$\theta = \sum_{i=1}^{k} \frac{\boldsymbol{u}_i^{\mathrm{T}}\boldsymbol{b}}{\sigma_i}\boldsymbol{v}_i + \sum_{i=p+1}^{m}(\boldsymbol{u}_i^{\mathrm{T}}\boldsymbol{b})\boldsymbol{v}_i. \tag{3.15}$$

The choice of k will be considered in detail later, but one possibility is to apply Picard's condition and truncate the expansion when $\boldsymbol{u}_i^{\mathrm{T}}\boldsymbol{b}/\sigma_i$ becomes large.

(*c*) *L-curves*

One way of obtaining the optimum value of the regularization parameter in the presence of correlated noise is to define an upper bound for the side constraint and minimize the residue,

$$\min_{\theta} \|\boldsymbol{A}\theta - \boldsymbol{b}\| \quad \text{subject to} \quad \|\boldsymbol{C}\theta - \boldsymbol{d}\| \leqslant \gamma, \tag{3.16}$$

or alternatively to set a limit for the residue and minimize the deviation from the side constraint,

$$\min_{\theta} \|\boldsymbol{C}\theta - \boldsymbol{d}\| \quad \text{subject to} \quad \|\boldsymbol{A}\theta - \boldsymbol{b}\| \leqslant \varepsilon. \tag{3.17}$$

Of course, the success of this approach is highly dependent on the physical insight of the analyst in determining the allowable constraint violation or measurement error (residue magnitude).

A different approach is to plot the norm of the side constraint, $\|\boldsymbol{C}\theta - \boldsymbol{d}\|$, against the norm of the residue, $\|\boldsymbol{A}\theta - \boldsymbol{b}\|$, obtained by minimizing the penalty function (3.3) for different values of λ. Hansen (1992) showed that the norm of the side constraint is a monotonically decreasing function of the norm of the residue, and any point (ε, γ) on the curve is a solution to the two constrained least-squares problems (3.16) and (3.17). He pointed out that for a reasonable signal-to-noise ratio and satisfaction of the Picard condition, the curve is approximately vertical for $\lambda < \lambda_{\mathrm{opt}}$, and soon becomes a horizontal line when $\lambda > \lambda_{\mathrm{opt}}$, with a corner near the optimal regularization parameter λ_{opt}. The curve is called the L-curve because of this behaviour. The optimum value of the regularization parameter λ_{opt} corresponds to the point with maximum curvature at the corner of the log-log plot of the L-curve. This point represents a balance between confidence in the measurements and the analyst's intuition.

(*d*) *Cross-validation*

The idea of cross-validation is to maximize the predictability of the model by choice of the regularization parameter λ. A predictability test can be arranged by omitting one data point, b_k, at a time and determining the best parameter estimate using the other data points, by minimizing (3.3). Then for each of the estimates, predict the missing data and find the value of λ that on average predicts the b_k best, in the sense of minimizing the cross-validation function

$$V_0(\lambda) = \frac{1}{n}\sum_{k=1}^{n}(b_k - \tilde{b}_k(\lambda))^2, \tag{3.18}$$

where $\tilde{b}_k(\lambda)$ is the estimate of b_k obtained from the remaining data. This is the method of cross-validation. According to Ahmadian *et al.* (1998), equation (3.18) is equivalent to

$$V_0(\lambda) = \frac{1}{n}\|[\mathrm{diag}(\boldsymbol{I} - \boldsymbol{R}(\lambda))]^{-1}[\boldsymbol{A}\theta(\lambda) - \boldsymbol{b}]\|^2, \tag{3.19}$$

where

$$\boldsymbol{R}(\lambda) = \boldsymbol{A}[\boldsymbol{A}^{\mathrm{T}}\boldsymbol{A} + \lambda^2\boldsymbol{C}^{\mathrm{T}}\boldsymbol{C}]^{-1}\boldsymbol{A}^{\mathrm{T}}, \tag{3.20}$$

and diag denotes the matrix with zeros assigned to the off-diagonal terms. Ordinary cross-validation has a rotational invariant version called generalized cross-validation (GCV); this is essentially a weighted version of (3.19) and is given by

$$V(\lambda) = \frac{n\|[\boldsymbol{A}\theta(\lambda) - \boldsymbol{b}]\|^2}{(\mathrm{trace}[\boldsymbol{I} - \boldsymbol{R}(\lambda)])^2}. \tag{3.21}$$

Table 5. *Natural frequencies* (Hz) *for the frame example*

mode	measured	initial	updated
1	226.8	269.5	221.5
2	275.2	287.7	270.9
3	537.4	615.0	537.0
4	861.5	928.7	861.7
5	974.8	1071.3	974.1

Ahmadian *et al*. (1998) give the background and further details. Equation (3.21) may be conveniently computed via the generalized SVD. Furthermore, the GCV based on the solution from the truncated generalized SVD may be defined as

$$V(k) = \frac{n\|[\boldsymbol{A}\theta(k) - \boldsymbol{b}]\|^2}{(n - m + p - k)^2}, \tag{3.22}$$

where k is the number of retained singular values and $\theta(k)$ is the corresponding solution.

(*e*) *An example of regularization*

The regularization methods were tested on the frame shown in figure 2. The frame was made from 25.4 mm square section aluminium tubing with 2.38 mm wall thickness. The frame was 584 mm long and 279 mm wide, and it contained four L-shaped welded joints and two T-joints that are difficult to model. Experimental data were obtained using standard hammer impact testing procedures on the freely suspended frame. The natural frequencies for the first 5 out-of-plane bending modes were identified, together with the corresponding mode shapes at the 13 locations shown in figure 2. Table 5 lists the measured natural frequencies. The structure was lightly damped and the real mode shapes were easily extracted.

A finite-element model was constructed to model the out-of-plane bending vibration of the frame. Each short beam was split into 4 elements and the longer beams split into 8 elements, giving a total of 28 beam or bar elements. Each of the 27 nodes had 3 degrees of freedom, producing a finite-element model with 81 degrees of freedom. The beam parts of the elements were Euler–Bernoulli beams, and the torsional contribution to the dynamics was also modelled. Table 5 lists the first five natural frequencies obtained from this model, and table 6 gives the modal assurance criterion (MAC) matrix. Although there is some error in the natural frequencies, the mode shape correlation is very good. It is also clear that the modes pair in natural frequency order. The measured modes were expanded using dynamic expansion to the full set of degrees of freedom of the finite-element model.

The model of the frame was updated using generic parameters, described earlier. The elements were split into five types shown in figure 3; namely, connecting elements, two types relating to each side of the L-joint, and two elements of the T-joints. Each element group has an associated set of 6 parameters per element, giving a total of 168 parameters in 30 groups. The values within two of the parameter groups are not changed, since these parameters would make the stiffness matrices of connecting elements different if the elements were rotated by 180°. Many models of the structure

Table 6. *The MAC matrix for the frame example*

		experimental mode number				
		1	2	3	4	5
	1	99.4	17.3	4.0	2.6	0.5
analytical	2	9.2	98.3	3.5	1.0	2.8
mode	3	0.0	0.1	99.5	4.3	1.4
number	4	2.7	1.7	1.1	99.7	2.7
	5	1.1	2.6	0.3	2.6	99.8

may be created, and the model we are using is not necessarily optimum; nevertheless, it will demonstrate the methods outlined in this paper. There are several ways of specifying the constraint that parameters corresponding to the equivalent generic parameter for elements within the same group should be approximately equal. We will focus on constraining three parameters to be approximately equal, requiring two independent constraints, as this is the smallest number that can be used for demonstration purposes. The following three examples of constraint matrix $\boldsymbol{C}$ all have the property that the constraint is exactly satisfied when all three parameters are equal:

$$\boldsymbol{C} = \begin{bmatrix} 1 & -1 & 0 \\ 0 & 1 & -1 \end{bmatrix}, \qquad \boldsymbol{C} = \begin{bmatrix} 2 & -1 & -1 \\ -1 & 2 & -1 \end{bmatrix}, \qquad \boldsymbol{C} = \begin{bmatrix} 1 & -1 & 0 \\ 0 & 1 & -1 \\ -1 & 0 & 1 \end{bmatrix}. \tag{3.23}$$

Indeed there are many more candidate constraint matrices as each of the above may be premultiplied by any non-singular matrix. Unfortunately, each of these choices of constraint matrix has a slightly different effect within the identification procedure, as the parameters are weighted slightly differently in the cost function (3.3). The third example has the advantage of symmetry in the effect on the parameters, but is not full rank. In terms of the penalty function, this constraint matrix (where $\boldsymbol{d} = \boldsymbol{0}$) minimizes the sum of the square differences between every pair of parameters. With m_g parameters within a group, there will be $m_g(m_g - 1)/2$ pairs of parameters, producing this number of rows in the constraint matrix. However, the matrix will still have rank $m_g - 1$. The equivalent full-rank constraint matrix may be computed easily via the SVD

$$\boldsymbol{C}^{\mathrm{T}}\boldsymbol{C} = \boldsymbol{U}\boldsymbol{\Sigma}\boldsymbol{U}^{\mathrm{T}}, \tag{3.24}$$

where $\boldsymbol{\Sigma}$ only contains the $m_g - 1$ non-zero singular values, and $\boldsymbol{U}$ contains the corresponding singular vectors. The new full-rank constraint matrix is then

$$\hat{\boldsymbol{C}} = \boldsymbol{\Sigma}^{1/2}\boldsymbol{U}^{\mathrm{T}}. \tag{3.25}$$

This constraint matrix is used in the updating of the frame.

The residual minimized in this example is given by

$$J(\theta) = \sum_{i=1}^{n_{\mathrm{mode}}} \|[-\omega_i^2\boldsymbol{M} + \boldsymbol{K}(\theta)]\phi_i\|^2 + W_{\mathrm{orthog}}^2|\phi_i^{\mathrm{T}}\boldsymbol{K}(\theta)\phi_i - \omega_i^2|^2, \tag{3.26}$$

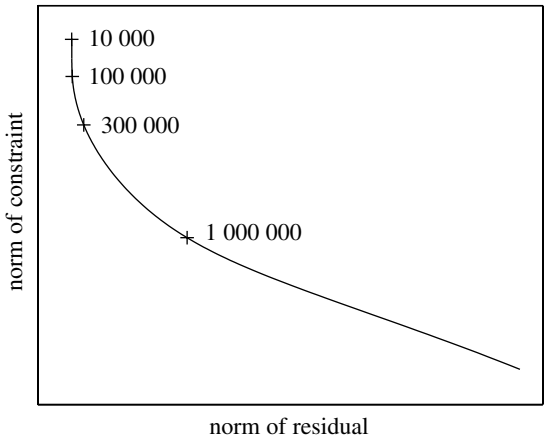

Figure 5. The L-curve for the frame example.

where ω_i and ϕ_i are the ith measured natural frequency and expanded mode shape (normalized with respect to the analytical mass matrix), n_{mode} is the number of modes measured, and only the stiffness matrix is a function of the vector of generic parameters θ. The first term minimizes the error in the eigenvalue equation. W_{orthog} is a weighting factor for the error in the stiffness orthogonality, and essentially weights the natural frequency error. In this example there are 405 equations (81 degrees of freedom for 5 modes) from the error in the eigenvalue equation, and a further 5 equations from the stiffness orthogonality. Thus $n = 410$ and $m = 140$. The orthogonality weighting factor W_{orthog} and the regulation parameter λ may both be changed, and the norms of the residual and constraint may be plotted to give a surface rather than the standard L-curve. For this example, L-curves were plotted for different values of W_{orthog} and engineering judgement was used to assess when the natural frequencies were given sufficient weight.

Figure 5 shows the L-curve as the regularization parameter λ is changed. There is a corner at a value of λ of approximately 3×10^5. Using the truncated SVD approach gives a similar L-curve (figure 6), and it shows that approximately 30 singular values should be retained. Using the generalized cross-validation function gives a defined minimum at 2.8×10^5 (figure 7), which is close to the value given by the L-curve. The updated natural frequencies based on this value for the regularization parameter (2.8×10^5) are shown in table 5. The MAC values for the updated model are not shown, as they are very similar to those of the initial model in table 6. Since the modes correlate well, even for the initial mode, it is not surprising that the MAC values do not improve. Finally, figure 8 shows the generalized cross-validation based on the truncated SVD, having a minimum at 44 singular values, although this minimum is not particularly marked.

4. Future developments

A major obstacle to obtaining updated models with physically meaningful parameters is that the structure of the *a priori* finite-element may not be correct. Model structure errors typically include the omission of important physical relationships, erroneous modelling of boundary conditions, mismodelling of joints, a nonlinear

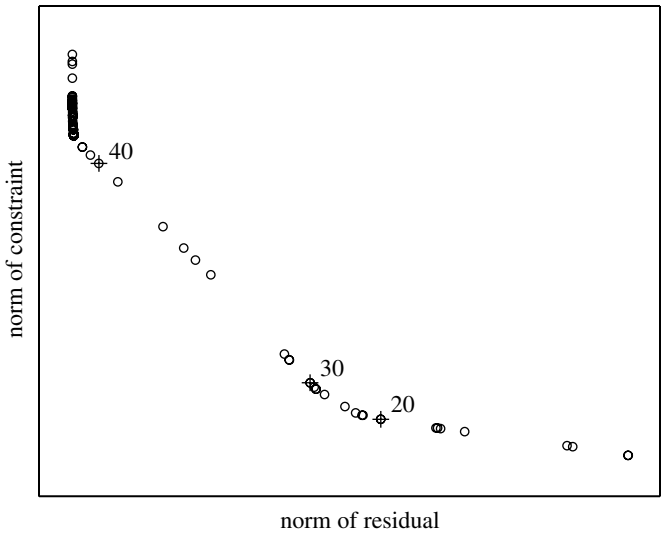

Figure 6. The L-curve for the frame example based on the truncated SVD.

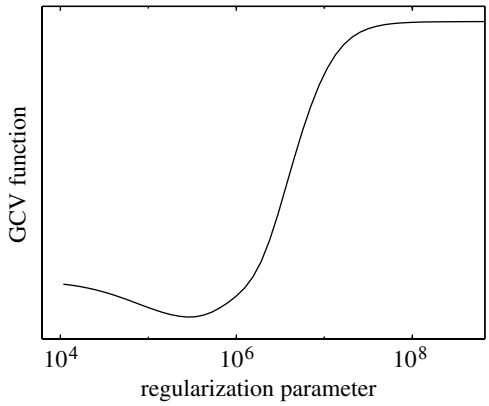

Figure 7. The generalized cross-validation function for the frame example.

structure assumed to be linear, and wrongly connected elements. This area of research now appears to be open for development, and new work close to 'model structure determination' includes methods of finite-element disassembly, the determination of finite-element connectivities, and inverse problems for chain-like finite-element structures.

Updating methods often rely on objective functions that are nonlinear in the unknown parameters. For example, the frequency response function sensitivities from a model which is condensed by using the so-called exact dynamic reduction will be unstable at frequencies close to the natural frequencies of the slave system with grounded masters. The penalty function based on the frequency domain output error constitutes a particularly difficult optimization problem with many local minima. A number of techniques including genetic algorithms, simulated annealing, neural networks and interval algorithms are becoming available to deal with these difficult optimization problems.

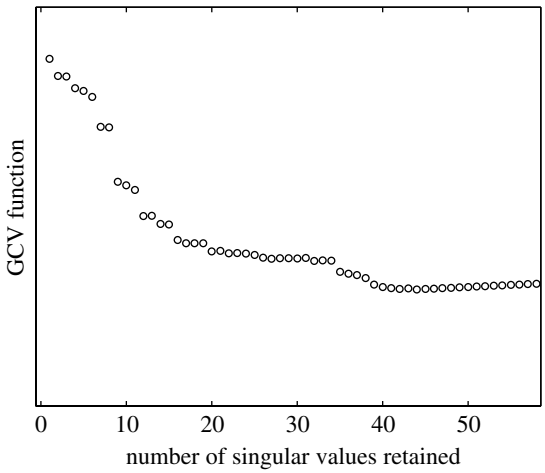

Figure 8. The generalized cross-validation function for the frame example based on the truncated SVD.

One way of reducing the number of updating parameters is to apply excitations which produce strong sensitivities to a subset of the parameters while causing the sensitivities to other parameters to vanish. The method of selective sensitivity requires the response predictions to a relatively large and possibly complex system of excitation forces (Ben-Haim 1994). The aim is to adapt the load system so that the output is sensitive to a selected set of parameters and insensitive to others. This is often possible because the substructure matrices have small rank and are very sparse. The physical difficulty of applying the required system of forces poses a serious problem to practical application, and further research is needed. Smart structures, with a large number of actuators distributed on a structure, may hold the key to applications of this technology.

Model updating has been a research topic for many years, but it has only recently been applied to large industrial problems. This may be due in part to some reluctance from finite-element analysts to changing the parameters in their models, because the changes seem to be very complex and comprehensive. This is perhaps the reason why the available commercial software has been written by vendors interested in the measurement of the vibration response, rather than the vendors of finite-element analysis software, even though the most sensible place for the updating software is within a finite-element package. There is a considerable computational burden associated with updating methods. Iterative schemes based on modal residuals will require the evaluation of the eigensolution for the structure many times. For a finite-element model with a large number of degrees of freedom this is not an insignificant task, although it is becoming less expensive on modern computer hardware. Industrial-scale updating problems have recently been solved and case studies performed. Typical examples include the recently completed BRITE project UPDYN (Irrgang 1997; Loureiro 1997).

The effect of uncertainty within a model, and how this uncertainty propagates through the model, is a topic that is just beginning to be addressed in the model updating and structural dynamics communities. For example, consider a structure that is manufactured to certain tolerances. If a prototype structure is tested, then the

model may predict the response for some set of parameters within the manufacturing tolerances. How should a model be validated in these circumstances? Propagating uncertainty does require huge computing resources that have only recently become affordable. However, this area will undoubtedly see an explosion of interest in the coming years.

It is difficult to determine the topics in model updating that will be active research areas in the future. Certainly more work is needed to determine the best way to parametrize a structure, with updating in mind. Alongside this parametrization, there will be continued improvement in methods of error localization and regularization (including the determination of weighting matrices) to cope with the ill-conditioning inherent in most updating methods. Powerful optimization methods will be applied to obtain the global minimum of nonlinear penalty functions. The methods will also be applied to many more industrial case studies.

5. Conclusion

This paper has outlined the authors' philosophy in dealing with two of the major issues in model updating, namely how to parametrize a structure and how to regularize the equations required to estimate the parameter values. Parameters should be chosen which have physical meaning but which are also able to model the errors in the finite-element model. Geometric parameters, generic elements and equivalent models were shown to have good features for model updating. Regularization based on physical considerations leads to updated models with physical meaning. Placing constraints on the parameters, such as minimizing the difference between nominally identical parameters, works very well. One difficulty with this approach is determining the relative weight given to the constraints, and this paper has proposed a number of approaches to determine this regularization parameter. A number of physical examples using experimental data have been described to show the effectiveness of the proposed approaches.

M.I.F. gratefully acknowledges the support of the EPSRC through the award of an advanced fellowship.

References

Ahmadian, H., Gladwell, G. M. L. & Ismail, F. 1997*a* Parameter selection strategies in finite element model updating. *J. Vib. Acoust.* **119**, 37–45.

Ahmadian, H., Mottershead, J. E. & Friswell, M. I. 1997*b* Parameterisation and identification of a rubber seal. In *Proc. 15th Int. Modal Analysis Conf., Orlando, FL*, pp. 142–146.

Ahmadian, H., Mottershead, J. E. & Friswell, M. I. 1998 Regularisation methods for finite element model updating. *Mech. Syst. Signal Process.* **12**, 47–64.

Ben-Haim, Y. 1994 Model updating of linear systems by selective sensitivity with deliberate structural modification. *Modal Analysis* **9**, 287–301.

Friswell, M. I. & Mottershead, J. E. 1995 *Finite element model updating in structural dynamics.* Dordrecht: Kluwer.

Friswell, M. I., Mottershead, J. E. & Ahmadian, H. 1998 Combining subset selection and parameter constraints in model updating. *J. Vib. Acoust.* **120**, 854–859.

Gladwell, G. M. L. & Ahmadian, H. 1995 Generic element matrices suitable for finite element model updating. *Mech. Syst. Signal Process.* **9**, 601–614.

Hansen, P. C. 1992 Analysis of discrete ill-posed problems by means of the L-curve. *SIAM Rev.* **34**, 561–580.

Hansen, P. C. 1994, Regularisation tools: a MATLAB package for analysis and solution of discrete ill-posed problems. *Numer. Algorithms* **6**, 1–35.

Hemez, F. M. & Farhat, C. 1995 Bypassing the numerical difficulties associated with the updating of finite element matrices. *AIAA Jl* **33**, 539–546.

Irrgang, A. (ed.) 1997 BRITE project UPDYN (P7666), task 7 final report, industrial tests: automotive.

Loureiro, R. (ed.) 1997 BRITE project UPDYN (P7666), task 8 final report, industrial tests: railway vehicle.

Mottershead, J. E. & Friswell, M. I. 1993 Model updating in structural dynamics: a survey. *J. Sound Vib.* **162**, 347–375.

Mottershead, J. E. & Friswell, M. I. (eds) 1998 Model updating. *Mech. Syst. Signal Process.* **12**(1).

Mottershead, J. E., Friswell, M. I., Ng, G. H. T. & Brandon, J. A. 1996 Geometric parameters for finite element model updating of joints and constraints. *Mech. Syst. Signal Process.* **10**, 171–182.